Concomitant alpha7 and beta2 nicotinic AChR subunit deficiency leads to impaired energy homeostasis and increased physical activity in mice

Somm, Emmanuel; Guerardel, Audrey; Maouche, Kamel; Toulotte, Audrey; Veyrat-Durebex, Christelle; Rohner-Jeanrenaud, Françoise; Maskos, Uwe; Hüppi, Petra Susan; Schwitzgebel Luscher, Valérie

How to cite

SOMM, Emmanuel et al. Concomitant alpha7 and beta2 nicotinic AChR subunit deficiency leads to impaired energy homeostasis and increased physical activity in mice. In: Molecular genetics and metabolism, 2014, vol. 112, n° 1, p. 64–72. doi: 10.1016/j.ymgme.2014.03.003

This publication URL: https://archive-ouverte.unige.ch//unige:40225
Publication DOI: 10.1016/j.ymgme.2014.03.003

Molecular Genetics and Metabolism 112 (2014) 64–72

Contents lists available at ScienceDirect

Molecular Genetics and Metabolism

journal homepage: www.elsevier.com/locate/ymgme

Concomitant alpha7 and beta2 nicotinic AChR subunit deficiency leads to impaired energy homeostasis and increased physical activity in mice

Emmanuel Somm [a,*], Audrey Guérardel [a], Kamel Maouche [b], Audrey Toulotte [a], Christelle Veyrat-Durebex [c], Françoise Rohner-Jeanrenaud [c], Uwe Maskos [d], Petra S. Hüppi [a], Valérie M. Schwitzgebel [a]

[a] Division of Development and Growth, Department of Paediatrics, Faculty of Medicine, University of Geneva, Geneva, Switzerland
[b] Université Paris-Diderot, Sorbonne-Paris-Cité, Laboratoire B2PE (Biologie et Pathologie du Pancréas Endocrine), Unité BFA (Biologie Fonctionnelle et Adaptative), CNRS UMR 8251, Paris, France
[c] Laboratory of Metabolism, Department of Internal Medicine Specialties, Faculty of Medicine, University of Geneva, Geneva, Switzerland
[d] Département de Neuroscience, Institut Pasteur, Unité Neurobiologie intégrative des systèmes cholinergiques, Paris, France

ARTICLE INFO

Article history:
Received 23 November 2013
Received in revised form 12 March 2014
Accepted 12 March 2014
Available online 19 March 2014

Keywords:
nAChR
Islet
Adipocyte
Obesity
Diabetes

ABSTRACT

Nicotinic acetylcholine receptors (nAChRs) are pentameric ligand-gated cation channels well characterized in neuronal signal transmission. Moreover, recent studies have revealed nAChR expression in nonneuronal cell types throughout the body, including tissues involved in metabolism. In the present study, we screen gene expression of nAChR subunits in pancreatic islets and adipose tissues. Mice pancreatic islets present predominant expression of α7 and β2 nAChR subunits but at a lower level than in central structures. Characterization of glucose and energy homeostasis in α7β2nAChR$^{-/-}$ mice revealed no major defect in insulin secretion and sensitivity but decreased glycemia apparently unrelated to gluconeogenesis or glycogenolysis. α7β2nAChR$^{-/-}$ mice presented an increase in lean and bone body mass and a decrease in fat storage with normal body weight. These observations were associated with elevated spontaneous physical activity in α7β2nAChR$^{-/-}$ mice, mainly due to elevation in fine vertical (rearing) activity while their horizontal (ambulatory) activity remained unchanged. In contrast to α7nAChR$^{-/-}$ mice presenting glucose intolerance and insulin resistance associated to excessive inflammation of adipose tissue, the present metabolic phenotyping of α7β2nAChR$^{-/-}$ mice revealed a metabolic improvement possibly linked to the increase in spontaneous physical activity related to central β2nAChR deficiency.

1. Introduction

The nicotinic acetylcholine receptors (nAChRs) consist of a wide family of ligand-gated cation channels opened by the binding of the endogenous neurotransmitter acetylcholine (ACh) or other biologic compounds including nicotine. nAChRs are formed by the symmetrical arrangement of five subunits around a central pore [1,2], resulting in many combinations since in mammals 16 nAChR subunits composing heteropentameric or homopentameric nAChRs have been discovered. The subunit composition of these receptors determines their expression pattern, function, and pharmacologic properties such as agonist sensitivity, desentizing period or ionic selectivity [3–5]. α7 subunits form homopentameric nAChRs with low agonist affinity, fast desensitization and high permeability to Ca^{2+} [3,4]. In contrast, β2 containing heteropentameric nAChRs present high agonist affinity and slow desensitization [3,4].

The widespread central and peripheral expressions of nAChRs make it difficult to study them in the context of regulation of energy homeostasis. Different central nicotinic cholinergic circuits involving at least α3, α4, α7, β2 and β4 nAChRs subunits regulate feeding through modulation of various hypothalamic orexigenic and anorexigenic neuropeptides [6]. Central nicotinic cholinergic signaling also regulates energy homeostasis through modulation of energy expenditure and control of spontaneous physical activity [6,7]. In this context, the β2nAChR$^{-/-}$ mice present an elevation in locomotor behavior but a dampened exploration behavior linked to alterations in the dopaminergic system [8–11]. In addition to these central roles in the brain, more subtle nAChR expression is detected in nonneuronal cell types throughout the body [12–14], suggesting a paracrine role for ACh. Functional binding of labeled nicotine, as well as detection of nAChRs in pancreatic islets and adipocyte [15–20] suggests that nicotinic cholinergic signaling in metabolic tissues can peripherally regulate energy homeostasis.

Nicotinic cholinergic stimulation improves the metabolic status of several genetic/environmental obese and diabetic rodent models [21]. In contrast, α7nAChR$^{-/-}$ mice present excessive adipose inflammation, impaired glucose tolerance and insulin resistance [22,23].

* Corresponding author at: Service of Endocrinology, Diabetology, and Metabolism, Centre Hospitalier Universitaire Vaudois/Department of Physiology, Rue du Bugnon 7, Lausanne CH-1005, Switzerland.
E-mail address: emmanuel.somm@chuv.ch (E. Somm).

http://dx.doi.org/10.1016/j.ymgme.2014.03.003
1096-7192/

In light of these recent reports, our present study aims 1) to screen gene expression of nAChR subunits in pancreatic islets and adipose tissues in wild-type mice and 2) to evaluate the metabolic impact of a double α7 and β2 nAChR deficiency in mice, focusing our attention on the regulation of glucose and energy homeostasis.

2. Materials and methods

2.1. Animal protocols

All animal procedures were approved by the "State of Geneva Veterinary Office" (Geneva, Switzerland). 6 month-old male α7β2nAChR$^{-/-}$ and wild-type C57Bl/6J mice (Charles River Laboratories, France) were housed in an environmentally-controlled room at the School of Medicine animal facility (Medical Center University, University of Geneva), in standard conditions (12 h light, 12 h dark cycle, temperature = 22 °C, hygrometry = 55 ± 10%), with free access to food (RM3 from Special Diet Services, Witham, Essex, UK) and water. Generation of double α7β2nAChR$^{-/-}$ mice resulted from breeding of single β2nAChR$^{-/-}$ and α7nAChR$^{-/-}$ mice for which genetic engineering was previously described [24,25].

Ad libitum food intake was measured by weighing the solid pellets placed in the grids on top of each cage during 5 consecutive days. For the fasting/refeeding experiment (involving glycemia, insulinemia, body weight and food intake monitoring), food pellets were removed for 6 h or 18 h prior to refeeding. The same cohort of α7β2nAChR$^{-/-}$ and wild-type C57Bl/6J mice underwent body composition analysis, the indirect calorimetry experiment, the fasting/refeeding experiment and the glucose homeostasis experiments with at least 1 week of recovery between each experiment. At sacrifice, epididymal white adipose tissues (eWAT) were weighed before being either fixed in paraformaldehyde (4%) or flash-frozen in liquid nitrogen before storage at −80 °C for later analyses.

2.2. Glucose homeostasis

Different physiological assays were performed to assess glucose homeostasis in α7β2nAChR$^{-/-}$ mice. For the 2-deoxyglucose (2-DG) tolerance test, after a 6 h fast, 2-DG (1 mg/g b.w.) in normal saline (0.9% NaCl) was administered intraperitoneally. Blood glucose and insulin levels were determined using tail blood at 0 and 10 min after 2-DG injection. For the glucose tolerance test (GTT), after a 6 h fast, glucose (2 mg/g b.w.) in normal saline (0.9% NaCl) was administered intraperitoneally. Blood glucose levels were determined using tail blood at 0, 15, 30, 60, 90 and 120 min after glucose injection and insulin levels were determined at 0, 15 and 120 min after glucose injection. For the pyruvate tolerance test (PTT), after a 6 h fast, pyruvate (2 mg/g b.w.) in normal saline (0.9% NaCl) was administered intraperitoneally. Blood glucose levels were determined using tail blood at 0, 15, 30, 60, 90 and 120 min after pyruvate injection. For the glucagon tolerance test, after a 6 h fast, glucagon (25 μg/kg b.w.) in normal saline (0.9% NaCl) was administered intraperitoneally. Blood glucose levels were determined using tail blood at 0, 15, 30, 60 min after glucagon injection. For the insulin tolerance test (ITT), after a 3 h fast, insulin (0.5 mU/g body weight; Actrapid, NovoNordisk, Bagsvaerd, Denmark) in normal saline (0.9% NaCl) was administered intraperitoneally. Blood glucose levels were determined using tail blood at 0, 15, 30, 60, and 90 min after insulin injection. Chemicals and reagents were provided by Sigma-Aldrich (St. Louis, MO, USA).

2.3. Body composition

Body composition, to dissociate lean, fat and bone compartments, was determined by DEXA (dual X-ray absorptiometry). The mice were anesthetized with intraperitoneal injections of ketamin (100 mg/kg) and xylazinhydrochlorid (rompum, 10 mg/kg) and scanned using a Lunar PIXImus densitometer (Lunar, Madison, WI). Calibration of the instrument was conducted before each run with an aluminum/lucite phantom provided by the manufacturer. Whole-body scans were analyzed using the software provided by the manufacturer. All data used for the analysis of body composition exclude the head and represent the subcranial body composition.

2.4. Indirect calorimetry and physical activity

Indirect calorimetry and spontaneous physical activity were monitored on α7β2nAChR$^{-/-}$ and wild-type C57BL/6J mice using the LabMaster system (TSE Systems GmbH, Berlin, Germany) in the Small Animal Phenotyping Facility (CMU, University of Geneva, Geneva), under standard laboratory conditions (22 ± 1 °C ambient temperature, light–dark cycle of 12/12 h, ad libitum food and water). Animals of both genotypes were housed in individual chambers for 5 days for acclimatization before starting the measurements with free access to food and water. Measurements were performed every 40 min during 48 h. For each time point, the measurements were averaged for each group. The calorimetry system is an open-circuit determining O_2 consumption (ml/kg/h), CO_2 production (ml/kg/h) and respiratory exchange rate (RER = VCO_2 / VO_2, where V is volume). Detection of animal location and movements was monitored by infrared sensor pairs arranged in strips, discriminating between horizontal (ambulatory) movements and vertical (fine exploration/rearing) movements, each of them occurring either in the central or the peripheral zone of the cage. Counts of activity were then added for each animal and averaged for each genotype.

2.5. Islet isolation

Human pancreatic islets were kindly provided by the University Hospital of Geneva (HUG), through the JDRF award 31-2008-413 (ECIT Islet for Basic Research Program). For mice islets, pancreata of male wild-type C57BL/6J mice (Charles River Laboratories, France) were immediately excised and cut into small pieces in Hanks solution before transfer into 5 ml of Hanks-collagenase type V solution (Sigma Aldrich, Buchs, Switzerland) incubated in a 37 °C water bath for 7 min. Digestion was stopped by addition of Hanks/BSA on ice and the pancreatic tissue was centrifuged several times before undigested fragments were carefully removed. After washing with Hank's solution, the tissue was concentrated into a pellet which was suspended on a Histopaque® 1077 gradient (Sigma Aldrich, Buchs, Switzerland). After centrifugation at 2500 rpm for 20 min, islets were harvested from the interface between the layers, washed and finally concentrated into pellets and immediately used for RNA extraction or cell culture.

2.6. Cell culture for insulin secretion

After isolation, islets were maintained in Krebs–Ringer bicarbonate HEPES buffer containing 0.1% BSA and 2.8 mmol/l glucose. Batches of 10 islets from α7β2nAChR$^{-/-}$ and wild-type C57BL/6J mice were handpicked and incubated in the presence of 22.8 mmol/l glucose for 1 h. Then, the supernatant was collected for insulin measurements using a mouse insulin Elisa kit (Mercodia, Uppsala, Sweden).

2.7. Blood measurements

For basal and challenged circulating glucose levels (during fasting/refeeding, 2-DG, GTT, ITT, PTT, Glucagon tolerance test), blood samples were collected by tail puncture for immediate glycemia measurement using a glucometer (Glucotrend Premium, Roche Diagnostics, Rotkreuz, Switzerland). For insulin and thyroid hormones measurements, blood was collected from a tail puncture, in heparinized tubes, placed on ice, centrifuged (3000 *g*, 10 min) and plasma was directly frozen before dosage using a mouse insulin Elisa kit (Mercodia, Uppsala, Sweden), a

Table 1
PCR primers for quantitative real-time PCR.

Specie	Target gene	Forward	Reverse
Human	Chrna1	5′-CAACCTAAAATGGAATCCAGATGA-3′	5′-CGCCAGATCTTTTCTGAAGGA-3′
Human	Chrna2	5′-GGTTCTCTGCATCCTTTCAATGA-3′	5′-TCTGCGAGGCTTCCTCTCA-3′
Human	Chrna3	5′-GCTGAAAATATGAAAGCACAAAATG-3′	5′-ACCATGGCAACATACTTCCAATC-3′
Human	Chrna4	5′-CCTGAAGGCCGAAGACACA-3′	5′-CCATGGCCACGTACTTCCA-3′
Human	Chrna5	5′-GTTTGATAATGCAGATGGACGTTT-3′	5′-ACAGTGCCATTGTACCTGATGACT-3′
Human	Chrna6	5′-GCCTGAAGTTGAAGATGTGATTAACA-3′	5′-TTCTACCTCCTTGGTTTCATTGTG-3′
Human	Chrna7	5′-GAATGGGACCTAGTGGGAATCC-3′	5′-GGCTCTTTGCAGCACTCATAGA-3′
Human	Chrna9	5′-TGCCGGCCTCAGAAAATG-3′	5′-AGGGCCATCGTGGCTATG-3′
Human	Chrna10	5′-GCCGCTCATCGGGAAGTAC-3′	5′-GAGTGCTGTTGAGAATGTGACCAT-3′
Human	Chrnb1	5′-CCGTCAGATCTTCATTCACAAACT-3′	5′-CGGGTTTGGGCCTTTTTAG-3′
Human	Chrnb2	5′-CGGCGTGCGCTTCATC-3′	5′-ACCATGGCGACGTACTTCCA-3′
Human	Chrnb3	5′-GAAAGAACATTTTATCAGCCAGGTAGTA-3′	5′-CACAGGAAGATTCGGTCAAGAAC-3′
Human	Chrnb4	5′-GCACATGAAGAATGACGATGAAG-3′	5′-CCACCACCATAGCCACGTACT-3′
Mice	Chrna1	5′-GGTGCGGAAGGTTTTTATCG-3′	5′-TCTCTGGATGGTCTTTTCATTGTG-3′
Mice	Chrna2	5′-TGCTGACTCTTCGGTGAAGGA-3′	5′-GCCAGAGGAAGATCCGGTCTA-3′
Mice	Chrna3	5′-GCTGAAAATATGAAAGCACAGAATG-3′	5′-ACCATGGCAACATACTTCCAATC-3′
Mice	Chrna4	5′-GAAGGCGTCCAGTACATTGCA-3′	5′-CCTTCACCGAGAAGTCTGTGTCT-3′
Mice	Chrna5	5′-TGGATCCCAGACATCGTTTTG-3′	5′-CGTACTGGCCCCTTCGAA-3′
Mice	Chrna6	5′-AAACATGAAGAGCCACAATGAAAC-3′	5′-CCACCATAGCCATGTATTTCCA-3′
Mice	Chrna7	5′-CAGCAGCTATATCCCCAATGG-3′	5′-GGCTCTTTGCAGCATTCATAGA-3′
Mice	Chrna9	5′-TGCCAGCCTCAGAAAACGT-3′	5′-GATCAAGGCCATGGTAGCTATGT-3′
Mice	Chrna10	5′-AGCATGCCACCTGCAGAGA-3′	5′-CTGTGGAGAATGTGACCATGGT-3′
Mice	Chrnb1	5′-CCGCCAGATCTTCATTCACA-3′	5′-GGGTTTGGGCCTCTTCAGA-3′
Mice	Chrnb2	5′-CGGACCATATGCGAAGTGAA-3′	5′-TGGCAACGTATTTCCAATCCT-3′
Mice	Chrnb3	5′-GAGGCATGTGAAGAAGGAACACT-3′	5′-TGAGCCACGAATTTCCAGTCT-3′
Mice	Chrnb4	5′-GTCGTCGACCGCCTGTTC-3′	5′-CCCCATGGTGCCCAGAA-3′
Mice	Il6	5′-CCTTCAGAGAGATACAGAAACTCTAATTCA-3′	5′-CTGTTAGGAGAGCATTGGAAATTG-3′
Mice	Tnf	5′-CAAAATTCGAGTGACAAGCCTGTA-3′	5′-CTCCAGCTGCTCCTCCACTT-3′
Mice	RPS29	5′-GCCAGGGTTCTCGCTCTTG-3′	5′-GGCACATGTTCAGCCCGTAT-3′

mouse/rat T3 total Elisa kit (T3043T-100) and a mouse/rat T4 total Elisa kit (T4044T-100) (Calbiotech, Spring valley, CA, USA).

2.8. RNA preparation and gene expression analysis

Total RNA from pancreatic islets and white/brown adipose tissues were extracted using the RNeasy Mini Kit® according to the manufacturer's protocol (Qiagen, Basel, Switzerland). One to five micrograms total RNA were reverse-transcribed using 400 units of Moloney Murine Leukemia Virus (MMLV) Reverse Transcriptase (Invitrogen, Basel, Switzerland), in the presence of 1 unit/μl RNAsin (Promega Corp, Madison, WI, USA), 0.2 μg random primers (oligo(dN)6) (Promega Corp, Madison, WI, USA), 2 mM dNTP and 20 μM DTT (Invitrogen, Basel, Switzerland). The expression of the cDNAs was determined by quantitative real-time PCR using an ABI StepOne Plus Sequence Detection System (Applera Europe, Rotkreuz, Switzerland) and were normalized using the housekeeping genes Ribosomal Protein S29. PCR products were quantified using the Master SYBR Green mix (Applera Europe, Rotkreuz, Switzerland) and results are expressed in arbitrary units (A.U) relative to the control group mean value or the predominantly expressed nAChR subunits. Primer sets (designed using the Primer Express software, Applera Europe, Rotkreuz, Switzerland) were tested for amplification efficiency (>90%) and were chosen when possible on both sides of an intron to avoid amplification of possible contaminating genomic DNA. The annealing temperature (60 °C) and amplicon size (50–150 bp) were automatically determined by the software. Oligos were used at 217 nM each (Microsynth, Switzerland). The sequence of the primers used is provided in Table 1.

2.9. Histological examination of adipose tissue

Epididymal white adipose tissue (eWAT) of $\alpha7\beta2nAChR^{-/-}$ and wild-type mice was fixed in a paraformaldehyde solution, embedded in paraffin, cut and stained with hematoxylin/eosin (H&E). Photographs were then taken using an Axiocam camera (Carl Zeiss, Gottingen, Germany) and the morphometric measurements were performed using the Image J software (Rasband W.S, ImageJ, NIH, Bethesda, MD, USA) as previously reported [26].

2.10. Statistics

Results are expressed as mean ± SEM for the indicated number of observations. One-way analysis of variance (ANOVA) and post-hoc analysis (using Student–Newman–Keuls) were performed using SigmaPlot11 (Systat Software). A p-value of <0.05 was considered statistically significant.

3. Results

3.1. α7 and β2 are the main nAChR subunits expressed in pancreatic islets of mice

The real-time quantitative PCR technique was used to screen the relative gene expression of α and β nAChR subunits in metabolic tissues. As in the hippocampus, a limbic part of the brain used as positive control (Figs. 1A and B), α7 and β2 were the nAChR subunits most predominantly expressed in pancreatic islets isolated from mice (Figs. 1C and D). In comparison, human pancreatic islets express predominantly α5 and β2 nAChR subunits (Figs. 1E and F). In mouse white (WAT) and brown (BAT) adipose tissue, α2 was the most expressed alpha nAChR subunit (Figs. 1G and I). Mice WAT expresses mainly β1 (Fig. 1J) whereas mice BAT expresses comparable amounts of β1 and β2 nAChR subunits (Fig. 1H). Nevertheless, peripheral nAChR expressions in pancreatic islets (Ct for β2 ≈ 29 cycles in mice; Ct for α5 and β2 ≈ 25 cycles in humans) as well as in fat pads (Ct for α2 ≈ 24 cycles; Ct for β1-β2 ≈ 24–25 cycles) are consistently lower when compared to central levels (Ct for α7 ≈ 20 and for β2 ≈ 22 in the mice hippocampus).

3.2. $\alpha7\beta2nAChR^{-/-}$ mice display no major defect in insulin secretion but present a lower glycemia

The predominant expression of α7 and β2 nAChR subunits in mice pancreatic islets led us to investigate whether these nAChR subunits

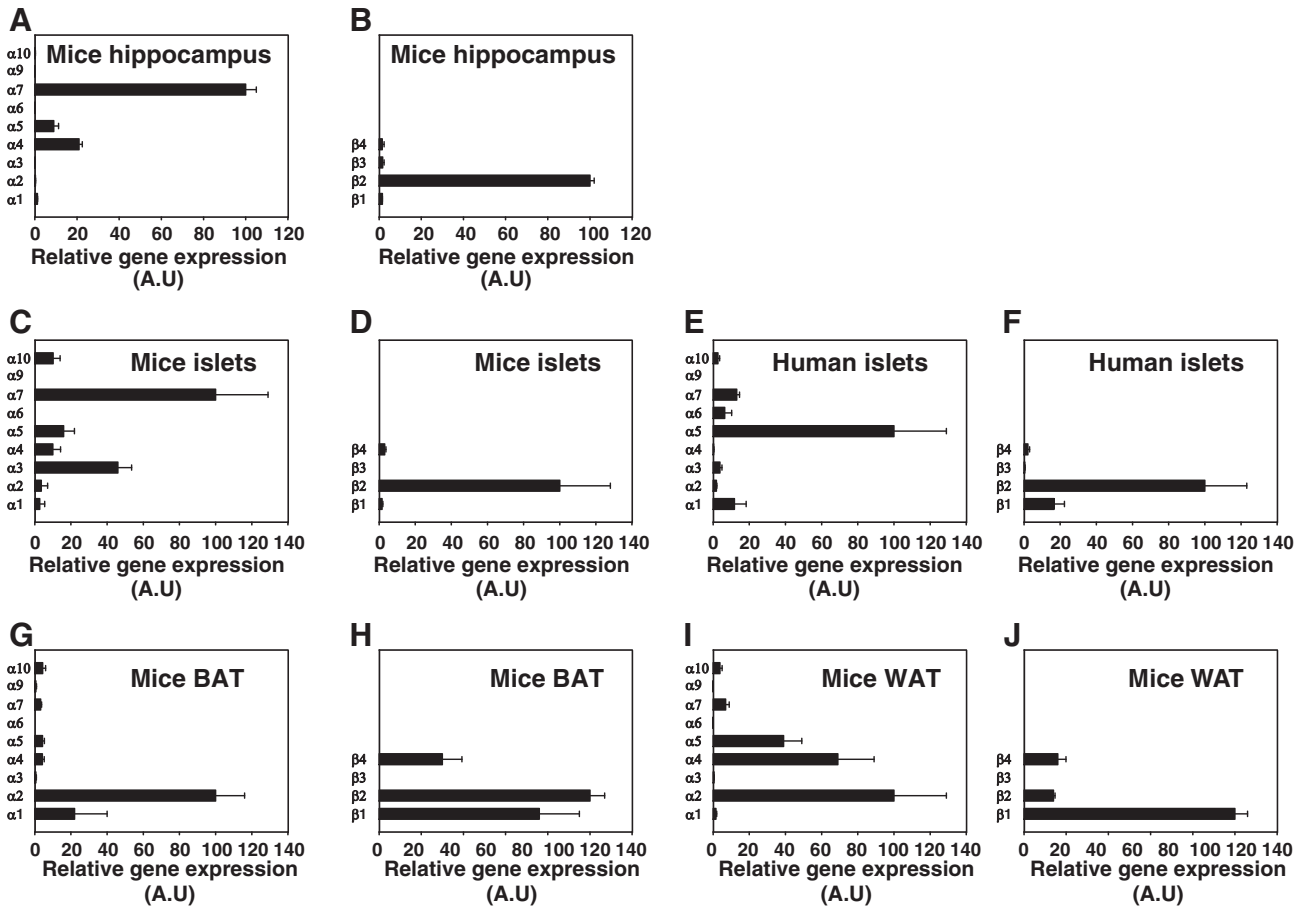

Fig. 1. Screening of nAChR subunits in pancreatic islets and adipose tissues. **A:** Relative gene expression for alpha nAChR subunits (arbitrary units, A.U) in mouse hippocampus. **B:** Relative gene expression for beta nAChR subunits (arbitrary units, A.U) in mouse hippocampus. **C:** Relative gene expression for alpha nAChR subunits (arbitrary units, A.U) in mouse pancreatic islets. **D:** Relative gene expression for beta nAChR subunits (arbitrary units, A.U) in mouse pancreatic islets. **E:** Relative gene expression for alpha nAChR subunits (arbitrary units, A.U) in human pancreatic islets. **F:** Relative gene expression for beta nAChR subunits (arbitrary units, A.U) in human pancreatic islets. **G**: Relative gene expression for alpha nAChR subunits (arbitrary units, A.U) in mouse BAT. **H**: Relative gene expression for beta nAChR subunits (arbitrary units, A.U) in mouse BAT. **I**: Relative gene expression for alpha nAChR subunits (arbitrary units, A.U) in mouse WAT. **J**: Relative gene expression for beta nAChR subunits (arbitrary units, A.U) in mouse WAT. Results are expressed as means ± SEM. $N = 6$ animals in panels A, B, G, H, I, and J. $N = 3$ pools of 2 animals in panel C and D. $N = 3$ human donors in panel E and F. List of primers used is given in Table 1.

could be involved in the regulation of glucose homeostasis and insulin secretion. To this aim, we studied the double α7β2nAChR$^{-/-}$ mouse model. Pancreas to body weight ratio was unchanged in α7β2nAChR$^{-/-}$ mice (Fig. 2A). After 6 h or 18 h of fasting, as well as 1 h following refeeding, insulinemia was not different in α7β2nAChR$^{-/-}$ in comparison to wild-type mice (Fig. 2B). In contrast, glycemia was decreased by 15 ± 3% ($p < 0.05$) in α7β2nAChR$^{-/-}$ mice (6 h) and by 11 ± 3% ($p < 0.05$) (18 h) following food removal but rose to similar levels as in wild-type mice 1 h after refeeding (Fig. 2C). We assessed the β-cell response to vagal stimulation using the administration of 2-deoxyglucose (2-DG) (a glucose analog that is not metabolized and blocks intracellular glucose utilization, promoting neuroglycopenia, vagus nerve stimulation and islet hormonal secretion). Insulinemia (Fig. 2D) and glycemia (Fig. 2E) were increased to the same extent in wild-type and in α7β2nAChR$^{-/-}$ mice 10 min following 2-DG administration, suggesting similar parasympathetic input in both genotypes. We also investigated potential consequences of α7 and β2 nAChR subunit deficiency on glucose-induced insulin secretion, both *in-vitro* (using isolated islets, Fig. 2F) and *in-vivo* (using intraperitoneal glucose tolerance test, Figs. 2G–I). *In-vitro*, pools of 10 islets from wild-type and α7β2nAChR$^{-/-}$ mice secreted comparable amounts of insulin in response to hyperglycemia (22.8 mM glucose concentration) (Fig. 2F). *In-vivo*, relative to basal glucose excursion during i.p. GTT was not modified in α7β2nAChR$^{-/-}$ compared to wild-type mice (Fig. 2G), confirmed by area under the curve values (Fig. 2H). Insulin secretion, expressed in absolute values (Fig. 2I), was similar in α7β2nAChR$^{-/-}$ and wild-type mice. Relative to basal glucose excursion during i.p. insulin tolerance test (Fig. 2J) and glucagon tolerance test (Fig. 2K) were globally similar between α7β2nAChR$^{-/-}$ and wild-type mice. During pyruvate tolerance test (Fig. 2L), relative to basal glucose levels were slightly increased 60 and 120 min after pyruvate administration in α7β2nAChR$^{-/-}$ mice. Taken together, these results show that double α7 and β2nAChR deficiency does not impact insulin secretion and insulin sensitivity, but dampens basal circulating glucose levels in the inter-meal interval or the fasted state without drastically reducing gluconeogenesis or glycogenolysis.

3.3. α7β2nAChR$^{-/-}$ mice display a defect in energy storage and modifications in food intake and body composition

Seeking to explain decreased basal glycemia unrelated to apparent modification in glycogen metabolism or insulin secretion/sensitivity, we further investigated energy homeostasis in α7β2nAChR$^{-/-}$ mice. At 6 months of age, body weight of α7β2nAChR$^{-/-}$ mice was not different from that of wild-type mice (Fig. 3A). Daily food intake was slightly increased by 10 ± 2% ($p < 0.05$) in α7β2nAChR$^{-/-}$ mice (Fig. 3B). α7β2nAChR$^{-/-}$ mice lost 39 ± 9% ($p < 0.05$) more weight than wild-type mice following a 18 h fasting period (Fig. 3C). Under ad libitum conditions, the α7β2nAChR$^{-/-}$ mice ate more than wild-type mice at different refeeding time points following the fasting period (Fig. 3D).

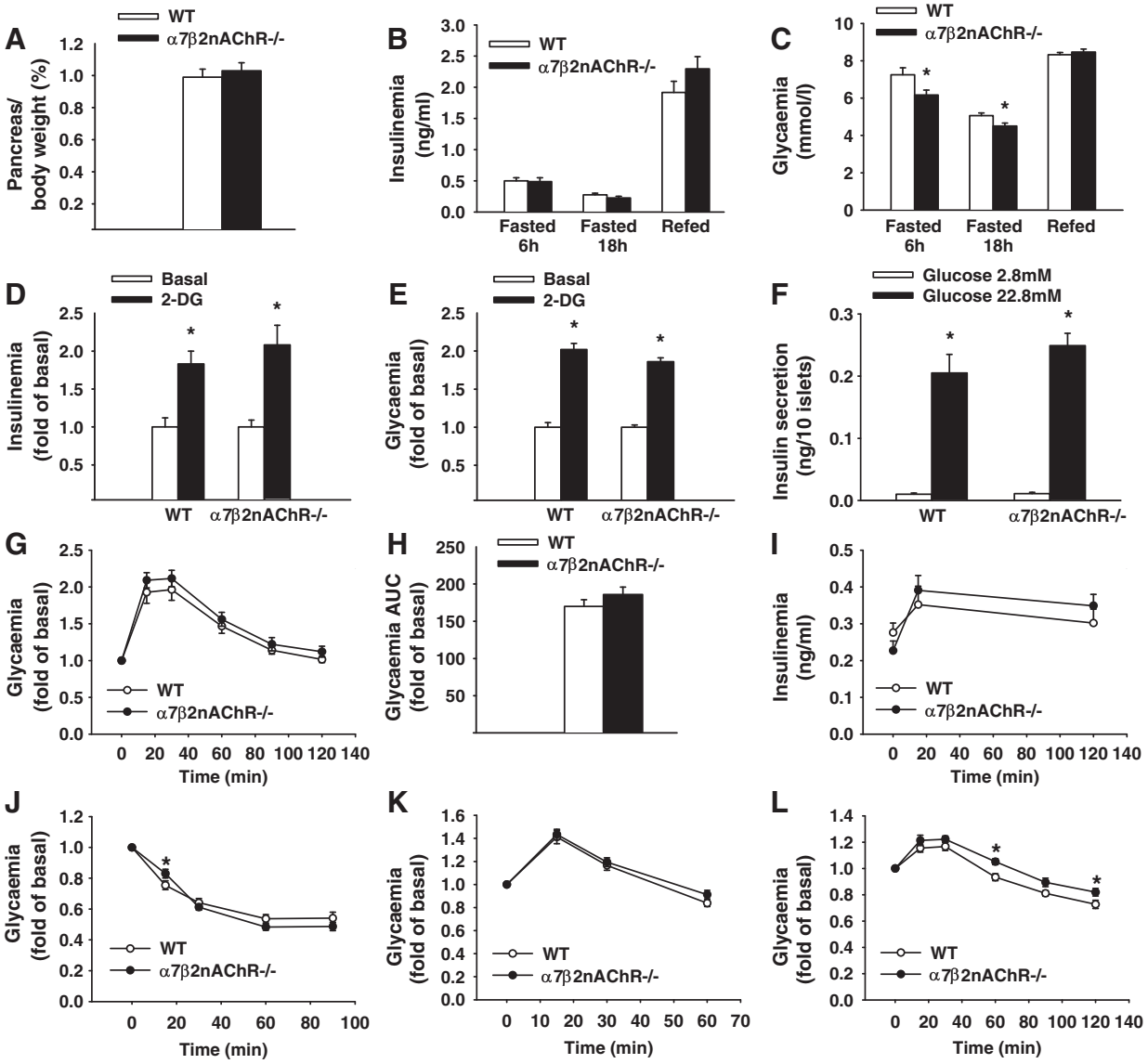

Fig. 2. Glucose homeostasis in $\alpha7\beta2nAChR^{-/-}$ mice. **A:** Relative weight of pancreas (% of body weight). **B:** Plasma insulin levels (ng/ml) in fasted or refed state. **C:** Plasma glucose levels (mmol/l) in fasted or refed state, $^{*}p < 0.05$ vs. corresponding wild-type group. **D:** Plasma insulin levels (fold of basal) after an i.p. administration of 2-DG. **E:** Plasma glucose levels (fold of basal) after an i.p. administration of 2-DG. **F:** Insulin secretion measured *in vitro* in isolated islets. Islets were incubated at 2.8 mmol/l glucose (basal) or 22.8 mmol/l glucose (stimulated), $^{*}p < 0.05$ vs. corresponding basal value of the same genotype. **G:** Plasma glucose levels (fold of basal) after an i.p. administration of glucose (glucose tolerance test). **H:** Plasma glucose levels area under the curve (fold of basal) after an i.p. administration of glucose (glucose tolerance test). **I:** Plasma insulin levels (ng/ml) after an i.p. administration of glucose (glucose tolerance test). **J:** Plasma glucose levels (fold of basal) after an i.p. administration of insulin (insulin tolerance test). **K:** Plasma glucose levels (fold of basal) after an i.p. administration of glucagon (glucagon tolerance test). **L:** Plasma glucose levels (fold of basal) after an i.p. administration of pyruvate (pyruvate tolerance test). Results are expressed as means ± SEM for $\alpha7\beta2nAChR^{-/-}$ (■) or wild-type (□) male mice. $N = 12$–16 animals in each group for panel A, B, D, E, G, H, I, J, K, L; $N = 25$–27 animals in each group for panel C; $N = 3$ independent experiments for panel F.

The greater weight loss during food unavailability led us to investigate body composition in $\alpha7\beta2nAChR^{-/-}$ mice by dual energy X-ray absorptiometry (DEXA). $\alpha7\beta2nAChR^{-/-}$ mice presented significantly increased lean body mass and a tendency to decreased body fat mass ($p = 0.06$) (Fig. 3E). In contrast, bone mass content was increased by 9 ± 2% ($p < 0.05$) in $\alpha7\beta2nAChR^{-/-}$ compared to wild-type mice (Fig. 3F). Both femur and subcranial whole body skeleton of $\alpha7\beta2nAChR^{-/-}$ mice showed elevated levels of mineral density compared to wild-type mice (Fig. 3G). Weight of epididymal fat pads was reduced by 51 ± 5% ($p < 0.05$) in $\alpha7\beta2nAChR^{-/-}$ compared to wild-type mice (Fig. 3H). Gene expression of pro-inflammatory cytokine TNF-α and IL-6 showed a non-significant trend to decrease in eWAT of $\alpha7\beta2nAChR^{-/-}$ mice (Fig. 3I). To determine the underlying mechanism involved in the limitation of eWAT accretion observed in $\alpha7\beta2nAChR^{-/-}$ mice, histological sections of eWAT were obtained from each genotype (Figs. 3J–K). Quantitative analysis of these sections (Fig. 3L) showed a decrease of 29 ± 7% ($p < 0.05$) in the size of the adipocyte from $\alpha7\beta2nAChR^{-/-}$ mice compared to those of wild-type mice, suggesting that hypotrophy of the adipocyte contributes to fat pad atrophy in $\alpha7\beta2nAChR^{-/-}$ mice.

A potential explanation for the unaltered body weight of $\alpha7\beta2nAChR^{-/-}$ mice and decreased fat storage despite their increased appetite might be an elevation in their energy expenditure. VO_2 consumption monitored on two consecutive days (Fig. 4A) was in fact increased in $\alpha7\beta2nAChR^{-/-}$ compared to wild-type mice [by 7 ± 2% ($p < 0.05$) during the dark phase (active period for rodents) and by 9 ± 2% ($p < 0.05$) during the light phase (resting period)] (Fig. 4B).

Elevation in VO_2 consumption was associated to an increase of 24 ± 6% in total T3 levels in $\alpha7\beta2nAChR^{-/-}$ mice (0.88 ± 0.04 ng/ml, $N = 15$) compared to wild-type mice (0.71 ± 0.03 ng/ml, $N = 16$, $p < 0.01$) whereas no change was observed in total T4 levels

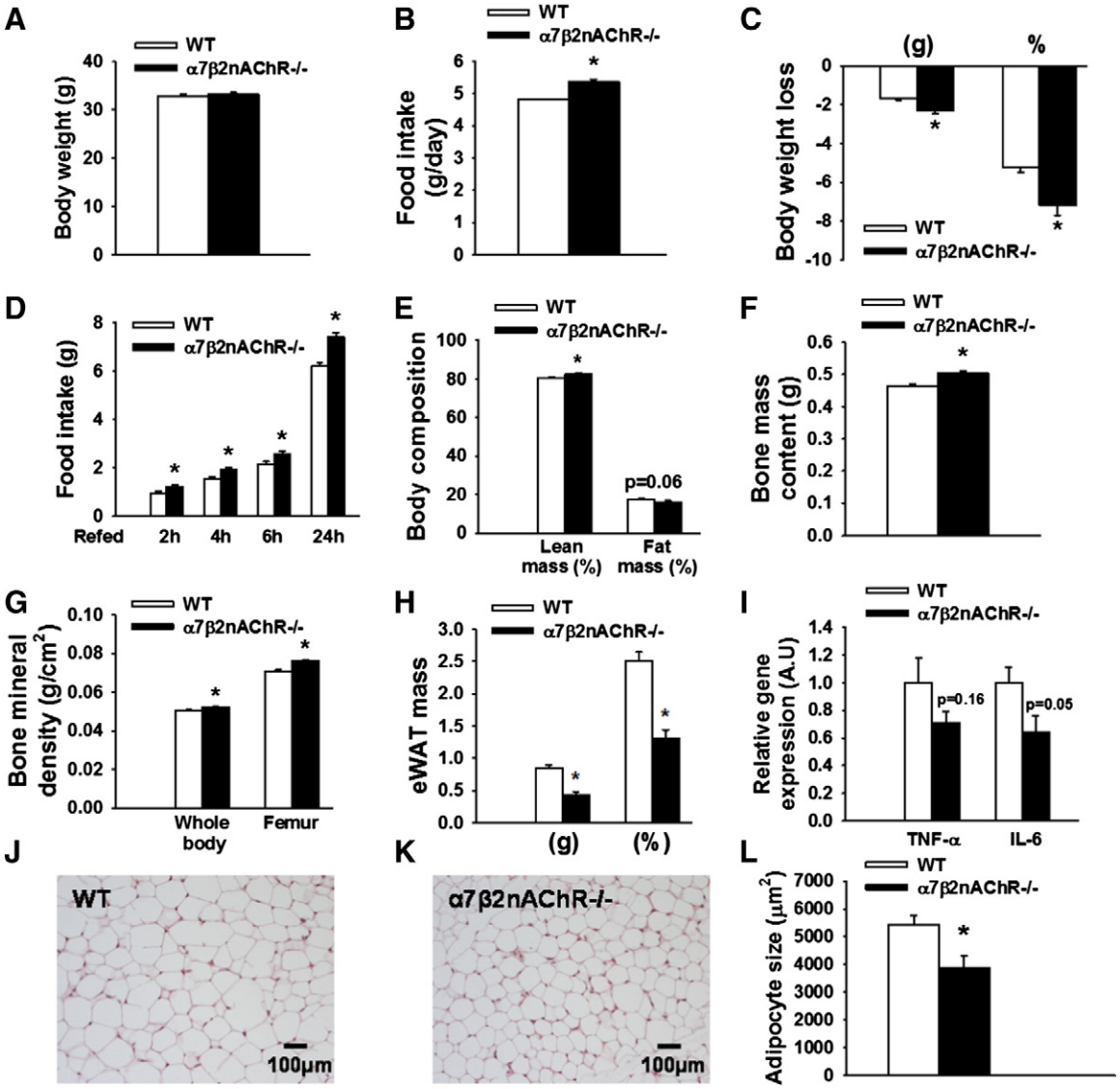

Fig. 3. Energy homeostasis in α7β2nAChR$^{-/-}$ mice. **A:** Body weight (g). **B:** Food intake (g/day), $^*p < 0.05$ vs. wild-type. **C:** Body weight loss after an 18 h-fasting period (in g or % of initial b.w.), $^*p < 0.05$ vs. wild-type. **D:** Food intake (g) after an 18 h-fasting period, $^*p < 0.05$ vs. wild-type. **E:** Body composition (lean mass and fat mass in %), $^*p < 0.05$ vs. wild-type. **F:** Bone mass content (g), $^*p < 0.05$ vs. wild-type. **G:** Bone mineral density (g/cm^2), $^*p < 0.05$ vs. wild-type. **H:** Epididymal white adipose tissue (eWAT) mass (in g or % of b.w.), $^*p < 0.05$ vs. wild-type. **I:** Relative gene expression of TNF-α and IL-6 in eWAT (A.U). **J:** Epididymal white adipose tissue (eWAT) histology of wild-type mice. **K:** Epididymal white adipose tissue (eWAT) histology of α7β2 nAChR$^{-/-}$ mice. **L:** Mean area of adipocytes (μm^2). Results are expressed as means ± SEM for α7β2 nAChR$^{-/-}$ (■) or wild-type (□) male mice. $N = 10$–12 animals in each group for panels A, B, C, D, H, and I; $N = 12$–16 animals in each group for panels E, F, and G. $N = 5$ animals in each group for panel L.

in α7β2nAChR$^{-/-}$ mice (1.29 ± 0.12 μg/dl) compared to wild-type mice (1.44 ± 0.24 μg/dl, $p = 0.58$) (data not shown). The altered adaptation to fasting previously observed in α7β2nAChR$^{-/-}$ mice (Fig. 3C) is corroborated by changes in energetic substrate use since the respiratory exchange ratio (RER = VCO_2/VO_2), was significantly reduced in α7β2nAChR$^{-/-}$ mice during the light phase (Fig. 4C), indicating that α7β2nAChR$^{-/-}$ mice oxidated more lipids than wild-type mice during this period. The circadian pattern of spontaneous physical activity was also assessed with the LabMaster system, allowing to discern horizontal (ambulatory) movements and vertical (fine exploration/rearing) movements, each of them occurring either in the central or the peripheral zone of the cage. Central ambulatory activity patterns appeared to be similar in α7β2nAChR$^{-/-}$ and wild-type mice (Fig. 4D). In contrast, central fine activity patterns appeared higher in α7β2nAChR$^{-/-}$ compared to wild-type mice (Fig. 4E). Summing these periodic movements, central activity was significantly increased by 22 ± 2% ($p < 0.05$) during the dark phase and by 37 ± 4% ($p < 0.05$) during the light phase in α7β2nAChR$^{-/-}$ mice, both times due to elevation in fine/rearing activity (Fig. 4F). In the same way, peripheral activity was significantly increased by 30 ± 2% ($p < 0.05$) during the dark phase and by 41 ± 3% ($p < 0.05$) during the light phase in α7β2nAChR$^{-/-}$ mice, always due to elevation in fine/rearing activity (Figs. 4G–I).

4. Discussion

In the present study, we investigated metabolic features of the double α7β2nAChR$^{-/-}$ mice. α7β2nAChR$^{-/-}$ mice present a moderate elevation in spontaneous food intake. Beyond nicotine anorectic action, nAChRs are well known to be involved in the regulation of food intake. In the lateral hypothalamus, neuronal networks express α4β2 and α7nAChRs [27–29] whereas α3β4 nAChRs seem rather implicated in both stimulation of POMC neurons [30] and inactivation of hypothalamic AMPK [31]. Surprisingly, the slight hyperphagia of α7β2nAChR$^{-/-}$ mice did not change their body weight but was associated with a modification of their body composition, with increased lean and bone mass

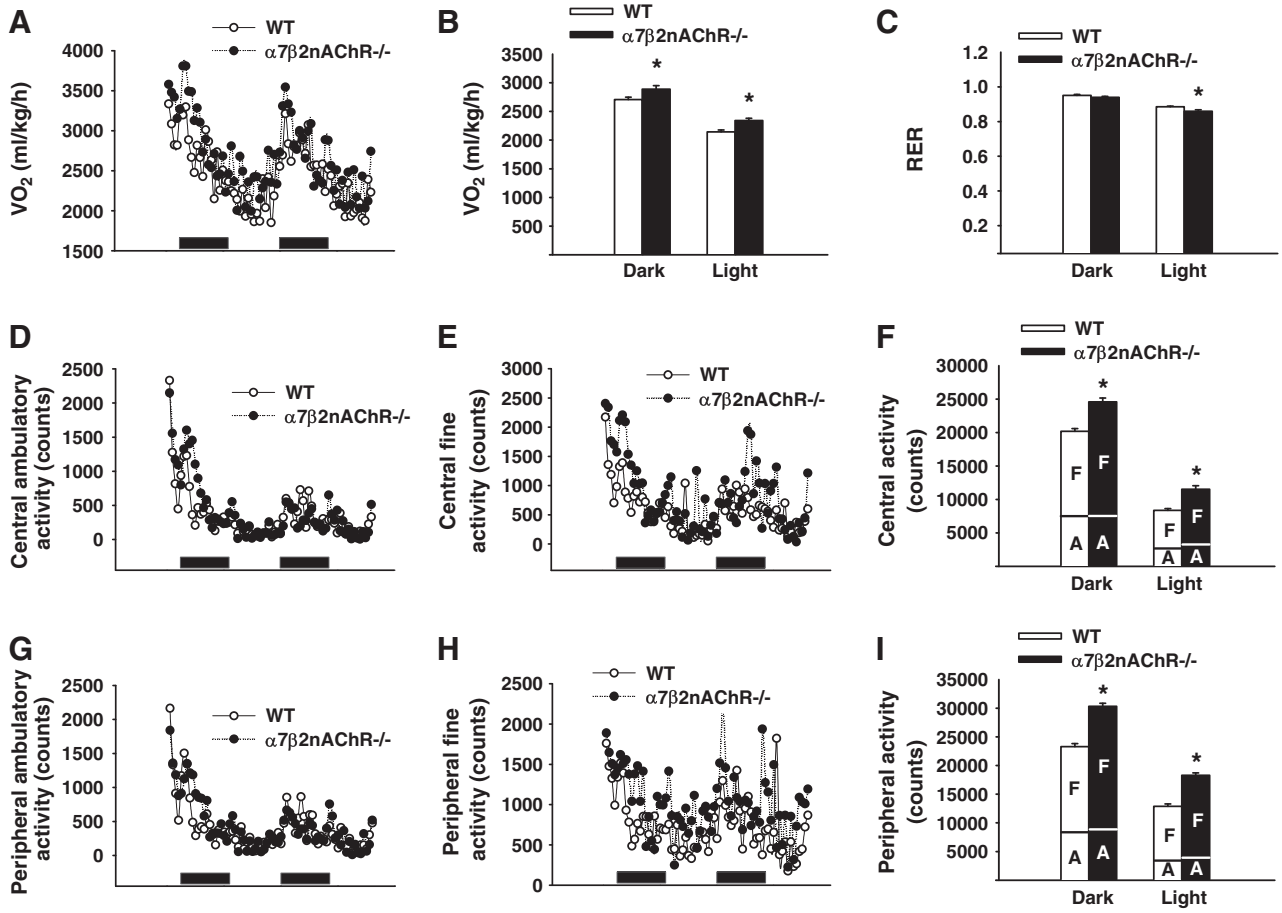

Fig. 4. Calorimetry and physical activity in $\alpha7\beta2nAChR^{-/-}$ mice. **A:** VO_2 consumption curves (ml/kg/h). **B:** VO_2 consumption mean values (ml/kg/h) during the dark or the light phase, $^*p < 0.05$ vs. wild-type. **C:** respiratory exchange ratio (RER = VCO_2/VO_2) during the dark or the light phase, $^*p < 0.05$ vs. wild-type. **D:** Central ambulatory activity curves (counts). **E:** Central fine activity curves (counts). **F:** Total central activity values (counts), $^*p < 0.05$ vs. wild-type. **G:** Peripheral ambulatory activity curves (counts). **H:** Peripheral fine activity curves (counts). **I:** Total peripheral activity values (counts), $^*p < 0.05$ vs. wild-type. Results are expressed as means ± SEM for $\alpha7\beta2nAChR^{-/-}$ (■) or wild-type (□) male mice. $N = 6$ animals in each group for all panels. SEM and significance not represented in panels A, D, E, G, and H to enhance lisibility. Panels F and I, legends inside the bars: F = fine, A = ambulatory.

and decreased fat pads, which can explain their increased sensitivity to fasting-induced weight loss.

Different explanations can be put forward concerning the limitation of fat accretion in $\alpha7\beta2nAChR^{-/-}$ mice.

First, this lean phenotype can be related to their elevation in energy expenditure. In fact, we observed a higher VO_2 consumption in $\alpha7\beta2nAChR^{-/-}$ compared to wild-type mice. As expected for nocturnal rodents, the activity was higher during the night period than during the light period in both genotypes. Nevertheless, $\alpha7\beta2nAChR^{-/-}$ mice present increased spontaneous physical activity when compared to wild-type mice. It clearly appeared that independently of the photoperiod (light/dark) and the location within the cage considered, the fine activity (corresponding to vertical exploration/rearing) mainly contributes to this increased spontaneous physical activity in $\alpha7\beta2nAChR^{-/-}$ mice. In contrast, the ambulatory activity (horizontal locomotion) was not drastically changed, except during the beginning of the first dark period, corresponding to introduction into the system and discovery of this novel environment. These observations supplement previous behavioral investigations linked to global nAChR deficiency. In fact, $\alpha7\beta2nAChR^{-/-}$ mice showed enhanced motor performance on the rotarod [32] and $\beta2nAChR^{-/-}$ mice were described as hyperreactive to novelty, suggesting that endogenous nAChR stimulation may exert a tonic control on monoamine-mediated locomotor responses [8]. Hyperactivity associated to β2nAChR deficiency appeared to be linked to selective dissociation of the high-order spatiotemporal organization of locomotor behavior (involving conflict resolution/social interaction) from low-level (more automatic motor behaviors) [9] and to the absence of specific inactive states (corresponding to decision moments) allowing to scan the environment and organize sequences of behavior [10]. Interestingly, hyperactivity of $\beta2nAChR^{-/-}$ mice can be normalized by selective expression of β2nAChR in the nigrostriatal and mesolimbic brain regions [11].

Besides the increased physical activity, the elevated level of T3, but not T4, also questions a possible mild hyperthyroidic status in $\alpha7\beta2nAChR^{-/-}$ animals. In this sense, further studies are required to investigate a possible nicotinic cholinergic control of desiodase activity.

In addition to the role of central nAChRs in regulation of food intake and physical activity, the lean phenotype of $\alpha7\beta2nAChR^{-/-}$ mice reported here could reflect a primary peripheral role for nAChRs in the biology of adipose tissue. We presently report that α2 nAChR is the most expressed alpha nAChR subunit in murine WAT and BAT, in adequation with both recent similar observations in mice [19] and with clinical associations between the rs2043063 SNP in the CHRNA2 gene and obesity [33]. We also detected low but relevant levels of α7 and β2nAChR mRNA in WAT and BAT. α7nAChRs appear to play an anti-inflammatory role in adipose tissue [22] and were shown to be downregulated in human obesity [20]. On the other hand, studies in $\beta2nAChR^{-/-}$ mice demonstrate that nAChRs containing the β2 subunit mediate transcription of adipokines in a depot-specific manner in WAT and BAT [19]. Future work involving tissue-specific knock-out mice models is nevertheless required to dissociate central and peripheral role of nAChR in adipose biology.

In the same way, functional binding of labeled nicotine, and detection of nAChRs in pancreatic islet cells [15–17] have suggested a local

role in these endocrine structures. The secretory activity of pancreatic islets is a highly regulated process, under the control of nutrition, hormones and the nervous system involving cholinergic signaling. The muscarinic receptor is classically described as the terminal effector of the cholinergic signaling in pancreatic β-cells [34–36] and the function of nAChRs in the context of pancreatic islets has long been limited to their role in ganglionic autonomic vagal neurotransmission [37–40]. Nevertheless, paracrine cholinergic signaling sensitizes the glucose-induced β-cell response in human islets [41] and nicotinic cholinergic stimulation dampens insulin secretion [15,42] whereas antagonism of the α7nAChR increases insulin release [43,44] according to previous studies.

We presently report that α7 and β2 are the nAChR subunits most predominantly expressed in pancreatic islets isolated from mice whereas α5 and β2nAChR subunits are prevalent in human islets, highlighting clinical associations between variants in the genes encoding these nAChR subunits with both insulin resistance and type 2 diabetes [45].

It can still be considered that nAChR expressions are subtle in pancreatic islets compared to central levels. Physiologically, α7β2nAChR$^{-/-}$ mice present no difference in basal insulinemia, as well as in glucose-induced and parasympathetically-mediated regulation of insulinemia in comparison to wild-type mice, ruling out a primordial role for these nAChR subunits in insulin secretion. α7β2nAChR$^{-/-}$ mice only exhibit reduced inter-meal and fasted glycemia compared to age-matched wild-type mice. Modifications in glycogenolysis or in gluconeogenesis were investigated to explain these decreased circulating glucose levels since chronic nicotine attenuates glycogenogenesis and gluconeogenesis in Zucker fatty (fa/fa) rats liver [46]. Neither sensitivity to glucagon nor neosynthesis of glucose from pyruvate appeared modified in α7β2nAChR$^{-/-}$ mice. Equally, sensitivity to insulin was not changed in α7β2nAChR$^{-/-}$ mice which was more surprising since the single knock-out α7nAChR$^{-/-}$ mouse is gluco-intolerant and resistant to insulin [22,23], due to inflammatory-prone status and increased adipose tissue infiltration by activated macrophages [22]. Unaltered insulin sensitivity in α7β2nAChR$^{-/-}$ mice presently observed is nevertheless consistent with the absence of excessive inflammation in their adipose tissue shown by unchanged TNF-α and IL-6 mRNA levels.

5. Conclusion

In the present study, we characterized the metabolic phenotype of mice deficient for both the α7 and β2nAChR subunits. Despite slight hyperphagia, body weight was unchanged in α7β2nAChR$^{-/-}$ mice which showed an increased bone accretion and reduced fat deposition. Unlike single knock-out α7nAChR$^{-/-}$ mice, the adipose tissue of α7β2nAChR$^{-/-}$ mice presented no evident sign of excessive inflammation. This fit phenotype of α7β2nAChR$^{-/-}$ mice could be linked to the elevated spontaneous physical activity associated to central deficiency in β2nAChR. The local role of nAChRs in adipose depot and pancreatic islet (a recent field of investigation which deserves further studies) could not be ruled out since various nAChR subunits are expressed in these metabolic tissues. Nevertheless, α7β2nAChR$^{-/-}$ mice showed no major defect in glucose homeostasis and insulin secretion, except for a reduced glycemia, possibly linked to their lean phenotype.

Disclosure statement

The authors have nothing to disclose.

Acknowledgments

We thank Laurent Depret and Damien Favrichon (Charles River FRANCE) for assistance in mice cohort management, Déborah Aeberhard for technical assistance, and Nicolas Bonnet and Serge Ferrari for access to DEXA measurement. Valérie M. Schwitzgebel received a research grant from the Gertrude von Meissner foundation and Emmanuel Somm was supported by the University of Geneva and the "Fondation pour Recherches Médicales (TULIPE)".

References

[1] E.X. Albuquerque, et al., Mammalian nicotinic acetylcholine receptors: from structure to function, Physiol. Rev. 89 (1) (2009) 73–120.
[2] J.P. Changeux, The nicotinic acetylcholine receptor: the founding father of the pentameric ligand-gated ion channel superfamily, J. Biol. Chem. 287 (48) (2012) 40207–40215.
[3] J. Lindstrom, Neuronal nicotinic acetylcholine receptors, Ion Channels 4 (1996) 377–450.
[4] R.C. Hogg, M. Raggenbass, D. Bertrand, Nicotinic acetylcholine receptors: from structure to brain function, Rev. Physiol. Biochem. Pharmacol. 147 (2003) 1–46.
[5] R. Hurst, H. Rollema, D. Bertrand, Nicotinic acetylcholine receptors: from basic science to therapeutics, Pharmacol. Ther. 137 (1) (2013) 22–54.
[6] M. Zoli, M.R. Picciotto, Nicotinic regulation of energy homeostasis, Nicotine Tob. Res. 14 (11) (2012) 1270–1290.
[7] U. Maskos, Role of endogenous acetylcholine in the control of the dopaminergic system via nicotinic receptors, J. Neurochem. 114 (3) (2010) 641–646.
[8] A.S. Villegier, et al., alpha7 and beta2 nicotinic receptors control monoamine-mediated locomotor response, Neuroreport 21 (17) (2010) 1085–1089.
[9] S. Granon, P. Faure, J.P. Changeux, Executive and social behaviors under nicotinic receptor regulation, Proc. Natl. Acad. Sci. U. S. A. 100 (16) (2003) 9596–9601.
[10] N. Maubourguet, et al., Behavioral sequence analysis reveals a novel role for beta2* nicotinic receptors in exploration, PLoS Comput. Biol. 4 (11) (2008) e1000229.
[11] M.E. Avale, et al., Interplay of beta2* nicotinic receptors and dopamine pathways in the control of spontaneous locomotion, Proc. Natl. Acad. Sci. U. S. A. 105 (41) (2008) 15991–15996.
[12] B.M. Conti-Fine, et al., Neuronal nicotinic receptors in non-neuronal cells: new mediators of tobacco toxicity? Eur. J. Pharmacol. 393 (1–3) (2000) 279–294.
[13] G. Sharma, S. Vijayaraghavan, Nicotinic receptor signaling in nonexcitable cells, J. Neurobiol. 53 (4) (2002) 524–534.
[14] L.C. Gahring, S.W. Rogers, Neuronal nicotinic acetylcholine receptor expression and function on nonneuronal cells, AAPS J. 7 (4) (2005) E885–E894.
[15] H. Yoshikawa, E. Hellstrom-Lindahl, V. Grill, Evidence for functional nicotinic receptors on pancreatic beta cells, Metabolism 54 (2) (2005) 247–254.
[16] M. Ohtani, et al., Mouse beta-TC6 insulinoma cells: high expression of functional alpha3beta4 nicotinic receptors mediating membrane potential, intracellular calcium, and insulin release, Mol. Pharmacol. 69 (3) (2006) 899–907.
[17] D.S. Delbro, Expression of the non-neuronal cholinergic system in rat beta-cells, Auton. Neurosci. 167 (1–2) (2012) 75–77.
[18] R.H. Liu, M. Mizuta, S. Matsukura, The expression and functional role of nicotinic acetylcholine receptors in rat adipocytes, J. Pharmacol. Exp. Ther. 310 (1) (2004) 52–58.
[19] A. Gochberg-Sarver, et al., Tnfα, Cox2 and AdipoQ adipokine gene expression levels are modulated in murine adipose tissues by both nicotine and nACh receptors containing the beta2 subunit, Mol. Genet. Metab. 107 (3) (2012) 561–570.
[20] R. Cancello, et al., The nicotinic acetylcholine receptor α7 in subcutaneous mature adipocytes: downregulation in human obesity and modulation by diet-induced weight loss, Int. J. Obes. (Lond). 36 (12) (2012) 1552–1557.
[21] E. Somm, Nicotinic cholinergic signaling in adipose tissue and pancreatic islets biology: revisited function and therapeutic perspectives, Arch Immunol Ther Exp (Warsz) 62 (2) (2014) 87–101.
[22] X. Wang, et al., Activation of the cholinergic antiinflammatory pathway ameliorates obesity-induced inflammation and insulin resistance, Endocrinology 152 (3) (2011) 836–846.
[23] T.Y. Xu, et al., Chronic exposure to nicotine enhances insulin sensitivity through alpha7 nicotinic acetylcholine receptor-STAT3 pathway, PLoS One 7 (12) (2012) e51217.
[24] M.R. Picciotto, et al., Abnormal avoidance learning in mice lacking functional high-affinity nicotine receptor in the brain, Nature 374 (6517) (1995) 65–67.
[25] A. Orr-Urtreger, et al., Mice deficient in the alpha7 neuronal nicotinic acetylcholine receptor lack alpha-bungarotoxin binding sites and hippocampal fast nicotinic currents, J. Neurosci. 17 (23) (1997) 9165–9171.
[26] E. Somm, et al., Prenatal nicotine exposure alters early pancreatic islet and adipose tissue development with consequences on the control of body weight and glucose metabolism later in life, Endocrinology 149 (12) (2008) 6289–6299.
[27] E. Wada, et al., Distribution of alpha 2, alpha 3, alpha 4, and beta 2 neuronal nicotinic receptor subunit mRNAs in the central nervous system: a hybridization histochemical study in the rat, J. Comp. Neurol. 284 (2) (1989) 314–335.
[28] P. Seguela, et al., Molecular cloning, functional properties, and distribution of rat brain alpha 7: a nicotinic cation channel highly permeable to calcium, J. Neurosci. 13 (2) (1993) 596–604.
[29] Y.H. Jo, D.A. Talmage, L.W. Role, Nicotinic receptor-mediated effects on appetite and food intake, J. Neurobiol. 53 (4) (2002) 618–632.
[30] Y.S. Mineur, et al., Nicotine decreases food intake through activation of POMC neurons, Science 332 (6035) (2011) 1330–1332.
[31] P.B. Martinez de Morentin, et al., Nicotine induces negative energy balance through hypothalamic AMP-activated protein kinase, Diabetes 61 (4) (2012) 807–817.

[32] L.M. Marubio, R. Paylor, Impaired passive avoidance learning in mice lacking central neuronal nicotinic acetylcholine receptors, Neuroscience 129 (3) (2004) 575–582.
[33] J. Kim, Association of CHRNA2 polymorphisms with overweight/obesity and clinical characteristics in a Korean population, Clin. Chem. Lab. Med. 46 (8) (2008) 1085–1089.
[34] I. Lundquist, Cholinergic muscarinic effects on insulin release in mice, Pharmacology 25 (6) (1982) 338–347.
[35] P. Gilon, J.C. Henquin, Mechanisms and physiological significance of the cholinergic control of pancreatic beta-cell function, Endocr. Rev. 22 (5) (2001) 565–604.
[36] I. Ruiz de Azua, et al., Critical metabolic roles of beta-cell M3 muscarinic acetylcholine receptors, Life Sci. 91 (21–22) (2012) 986–991.
[37] J.I. Stagner, E. Samols, Modulation of insulin secretion by pancreatic ganglionic nicotinic receptors, Diabetes 35 (8) (1986) 849–854.
[38] B. Ahren, G.J. Taborsky Jr., The mechanism of vagal nerve stimulation of glucagon and insulin secretion in the dog, Endocrinology 118 (4) (1986) 1551–1557.
[39] S. Nishi, et al., Vagal regulation of insulin, glucagon, and somatostatin secretion in vitro in the rat, J. Clin. Invest. 79 (4) (1987) 1191–1196.
[40] A.L. Kirchgessner, M.T. Liu, Immunohistochemical localization of nicotinic acetylcholine receptors in the guinea pig bowel and pancreas, J. Comp. Neurol. 390 (4) (1998) 497–514.
[41] R. Rodriguez-Diaz, et al., Alpha cells secrete acetylcholine as a non-neuronal paracrine signal priming beta cell function in humans, Nat. Med. 17 (7) (2011) 888–892.
[42] M. Ohtani, J.W. Daly, T. Oka, Co-existence of muscarinic and nicotinic receptors and their functional interaction in mouse Beta-TC6 cells, Eur. J. Pharmacol. 604 (1–3) (2009) 150–157.
[43] K. Ejiri, H. Taniguchi, S. Baba, Participation of nicotinic receptor in hormone release from isolated rat islets of Langerhans, Diabetes Res. Clin. Pract. 6 (1) (1989) 53–59.
[44] K. Ejiri, et al., Possible involvement of cholinergic nicotinic receptor in insulin release from isolated rat islets, Diabetes Res. Clin. Pract. 8 (3) (1990) 193–199.
[45] J. Yang, et al., A gene-family analysis of 61 genetic variants in the nicotinic acetylcholine receptor genes for insulin resistance and type 2 diabetes in American Indians, Diabetes 61 (7) (2012) 1888–1894.
[46] R.H. Liu, M. Mizuta, S. Matsukura, Long-term oral nicotine administration reduces insulin resistance in obese rats, Eur. J. Pharmacol. 458 (1–2) (2003) 227–234